Available online at www.sciencedirect.com
ScienceDirect
ELSEVIER
Finite Elements in Analysis and Design 42 (2006) 1240–1247
FINITE ELEMENTS IN ANALYSIS AND DESIGN
www.elsevier.com/locate/finel

A 2D field-consistent beam element for large displacement analysis using the total Lagrangian formulation

P. Nanakorn*, L.N. Vu

School of Civil Engineering and Technology, Sirindhorn International Institute of Technology, Thammasat University, PO Box 22, Thammasat-Rangsit Post Office, Pathumthani 12121, Thailand

Received 15 December 2005; received in revised form 9 May 2006; accepted 13 June 2006
Available online 31 July 2006

Abstract

In this study, a new 2D Euler–Bernoulli beam element for large displacement analysis using the total Lagrangian formulation is proposed. In large displacement analysis, the beam kinematics written based on the total Lagrangian description is complicated. As a result, it is not easy to find suitable interpolations that are field consistent for beam elements developed in this description. For this reason, existing total Lagrangian beam elements generally employ field-inconsistent interpolations, which result in degradation of element performances. In this study, field-consistent interpolations for a 2D Euler–Bernoulli beam element are proposed. The field consistency is obtained by using a set of interpolations that satisfy a required relationship between relevant displacement fields. The construction of the interpolations is made possible by allowing the interpolations to be expressed as nonlinear functions of nodal degrees of freedom. The validity and efficiency of the proposed element are shown by solving various numerical examples found in the literature.

Keywords: Beam elements; Total Lagrangian formulation; Large displacement analysis; Geometrical nonlinearity

1. Introduction

Several beam finite elements for large displacement analysis have been proposed by many researchers [1–12]. It may be said that there are in essence three main aspects in the development of this type of beam element. These aspects are the reference configuration, the beam kinematics and the approximation of the displacement fields. The choice of reference configuration depends on the choice of kinematic description. Three kinematic descriptions in current use are the total Lagrangian description, the updated Lagrangian description, and the co-rotational description. In this paper, the last aspect of the three aforesaid main aspects—the approximation of the displacement fields—for 2D beams described based on the total Lagrangian description is discussed. In fact, in this study, a new 2D Euler–Bernoulli beam element for large displacement analysis with small strains derived based on the total Lagrangian description is proposed. The focus of the development of the proposed element is on creating displacement interpolations that are field consistent even when displacements are large. It is known that various interpolation functions have been used in linear and geometrically nonlinear beam elements. These interpolation functions are defined based on various types of nodal degree of freedom [1,2,6,8,9,11]. Nodal degrees of freedom employed can be a set of translational displacements [1,9], a set of rotational displacements [6], a set of translational and rotational displacements [2,8], or even a set of curvatures [11]. In case of 3D linear beam elements, it is common that the axial and transverse displacements together with the axial and transverse rotations are used as nodal degrees of freedom. Under the assumption of small displacements used in linear beam analysis, the transverse rotation and the transverse displacement of the same bending plane are dependent. In linear Euler–Bernoulli beam elements, which do not consider shear deformations, the dependency between the transverse rotation and the transverse displacement of each bending plane is generally considered during the construction of the interpolation functions. In other words, the transverse rotation and the transverse displacement of each bending plane are expressed in forms that satisfy the

* Corresponding author. Tel.: +662 986 9009x1906; fax: +662 986 9009x1900.
E-mail address: nanakorn@siit.tu.ac.th (P. Nanakorn).

0168-874X/$ - see front matter © 2006 Elsevier B.V. All rights reserved.
doi:10.1016/j.finel.2006.06.002

dependent relationship between them. As a result, field-consistent interpolations are obtained. On the contrary, in linear Timoshenko beam elements, which consider shear deformations, this field dependency is normally neglected as a result of independent approximations for the transverse rotation and the transverse displacement of the same bending plane. The field-inconsistent interpolations in linear Timoshenko beam elements result in a well-known phenomenon called shear locking where inaccurately stiff solutions are obtained. It is possible, however, to remove the field inconsistency in linear Timoshenko beam elements by using appropriate interpolation functions [13,14]. One other possibility to achieve the field consistency for linear beam elements, while still considering shear deformations, is to employ the laminated beam theory [15].

In case of geometrically nonlinear beam elements with small strains that employ the total Lagrangian formulation, nodal degrees of freedom are described with respect to a fixed reference frame that is defined at the initial configuration. This fixed reference frame is normally defined by using coordinate axes that are aligned with the longitudinal axis and the two orthogonal bending directions of the beam at its initial configuration. With the reference frame defined as such, the displacements and the rotations in the directions of the coordinate axes are still mostly used as nodal degrees of freedom. Due to large displacements, the longitudinal displacement, the transverse displacements and the transverse rotations become complicatedly dependent on each other. As a result, it becomes difficult to find a set of interpolation functions that are field consistent. To obtain field-consistent interpolations, the interpolations for these translational displacements and rotations must satisfy the complicated relationships between these interpolated fields. One practical interpolation technique used in the total Lagrangian beam elements is to approximate displacements at a point from displacements of points on nodal cross-sections that have the same projected position as the point of interest [16–18]. This technique often employs standard polynomial interpolation functions. As a result, the displacements are interpolated from the values of nodal displacements and the values of nonlinear functions of nodal rotations. This interpolation technique, unfortunately, does not yield field-consistent interpolations.

When the updated Lagrangian formulation is used in large displacement analysis with small strains, the problem of field inconsistency may be avoided. This is true when the displacements from the last reference configuration to the next configuration are small and appropriate interpolation functions are used. Accordingly, the Euler–Bernoulli interpolation functions for small displacement analysis are sometimes used in beam elements derived with the updated Lagrangian formulation without any modification [5,12,19]. Note that, with the updated Lagrangian formulation, the problem of field inconsistency will arise every time the displacements from the last reference configuration to the next configuration are not small. The co-rotational formulation [3,7,8,20,21] can also avoid the problem of field inconsistency when it is used in large displacement analysis with small strains. This is because the basic concept of the formulation is to decompose the displacements into a portion of large rigid displacements and a portion of small displacements due to small deformations. The interpolation functions are consequently used for the small displacements. If appropriate interpolation functions are used, there will be no problem of field inconsistency. A comparative discussion on beam elements derived with the total Lagrangian and co-rotational formulations can be found in the work by Pacoste and Eriksson [22].

This paper presents an approach to handle the problem of field inconsistency found in 2D beam elements for large displacements with small strains derived with the total Lagrangian formulation. The proposed beam element is derived based on the Euler–Bernoulli beam assumptions. The derivation of the proposed beam element is straightforward and does not involve any complicated concepts or assumptions. To tackle the problem of field inconsistency, it is natural that required relationships among interdependent fields are considered and satisfied. The interdependent fields cannot be independently interpolated. Instead, interpolations of all interdependent fields must be considered together. In this study, the field consistency is obtained by finding a set of interpolations that satisfy a required relationship between relevant displacement fields in the proposed 2D beam element. The construction of the displacement interpolations becomes possible by appropriately allowing the interpolations to be expressed as nonlinear functions of nodal degrees of freedom. The validity and efficiency of the proposed element are shown by using various numerical examples found in the literature.

2. Kinematics of an Euler–Bernoulli beam with large displacements

Consider a section of a beam shown in Fig. 1. Due to the deformation of the beam, a particle at $P_0(X, Y)$ in the original configuration $\mathscr{C}_0$ moves to $P(x, y)$ in the current configuration $\mathscr{C}$. Under the assumptions of the Euler–Bernoulli beam, the following relations can be obtained:

$$x = X + u_X - Y \sin\theta, \tag{1}$$

$$y = u_Y + Y \cos\theta, \tag{2}$$

where u_X and u_Y are the displacements of the projection of $P_0(X, Y)$ on the neutral axis in the XY system. In addition, θ represents the rotation of the cross-section.

Denote s as the arc length along the neutral axis in the current configuration. The following relations can then be obtained:

$$1 + u'_X = s' \cos\theta, \quad u'_Y = s' \sin\theta, \tag{3}$$

$$\cos\theta = \frac{1 + u'_X}{\sqrt{(1 + u'_X)^2 + (u'_Y)^2}}, \tag{4}$$

$$\sin\theta = \frac{u'_Y}{\sqrt{(1 + u'_X)^2 + (u'_Y)^2}}, \tag{5}$$

$$\tan\theta = \frac{u'_Y}{1 + u'_X}, \tag{6}$$

where primes denote the derivatives with respect to X. Note that Eqs. (4)–(6) represent a dependent relationship between

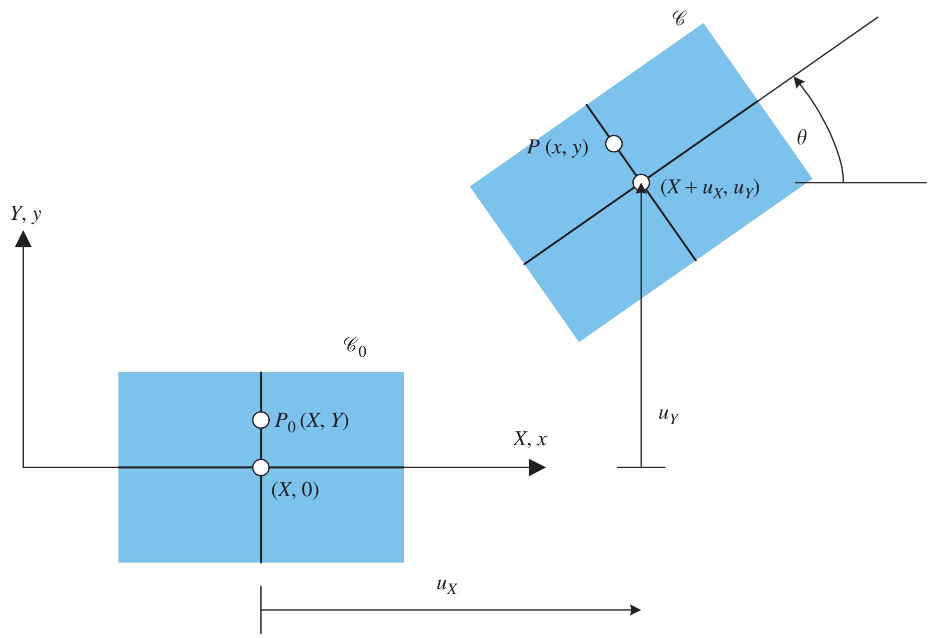

Fig. 1. Euler–Bernoulli beam with large displacements.

u_X, u_Y and θ that must be satisfied by the interpolations in order to obtain the field consistency. Note further that, for small displacements, Eq. (6) becomes $\theta = u'_Y$.

By using Eqs. (1) and (2), the deformation gradient matrix is written as

$$\mathbf{F} = \begin{bmatrix} \dfrac{\partial x}{\partial X} & \dfrac{\partial x}{\partial Y} \\ \dfrac{\partial y}{\partial X} & \dfrac{\partial y}{\partial Y} \end{bmatrix} = \begin{bmatrix} 1 + u'_X - Y\theta' \cos\theta & -\sin\theta \\ u'_Y - Y\theta' \sin\theta & \cos\theta \end{bmatrix}. \tag{7}$$

The deformation gradient matrix is used to compute the Green strain matrix as

$$\mathbf{E} = \begin{bmatrix} E_{XX} & E_{XY} \\ E_{YX} & E_{YY} \end{bmatrix} = \frac{1}{2}(\mathbf{F}^{\mathrm{T}}\mathbf{F} - \mathbf{I}). \tag{8}$$

Introduce an orthogonal matrix $\mathbf{R}$ defined as

$$\mathbf{R} = \begin{bmatrix} \cos\theta & \sin\theta \\ -\sin\theta & \cos\theta \end{bmatrix}. \tag{9}$$

Define a matrix $\bar{\mathbf{F}}$ as

$$\bar{\mathbf{F}} = \mathbf{RF} = \begin{bmatrix} (1 + u'_X)\cos\theta + u'_Y \sin\theta - Y\theta' & 0 \\ 0 & 1 \end{bmatrix}. \tag{10}$$

Note that from Eq. (3)

$$-(1 + u'_X)\sin\theta + u'_Y \cos\theta = 0. \tag{11}$$

With help of Eq. (3), write $\bar{\mathbf{F}}$ as

$$\bar{\mathbf{F}} = \mathbf{I} + \mathbf{L}, \tag{12}$$

where

$$\mathbf{L} = \begin{bmatrix} (s' - 1) - Y\theta' & 0 \\ 0 & 0 \end{bmatrix}. \tag{13}$$

Since $\mathbf{R}$ is orthogonal, the Green strain $\mathbf{E}$ can be rewritten as

$$\mathbf{E} = \tfrac{1}{2}(\bar{\mathbf{F}}^{\mathrm{T}}\bar{\mathbf{F}} - \mathbf{I}) = \tfrac{1}{2}(\mathbf{L} + \mathbf{L}^{\mathrm{T}} + \mathbf{L}^{\mathrm{T}}\mathbf{L}) \approx \tfrac{1}{2}(\mathbf{L} + \mathbf{L}^{\mathrm{T}}) = \mathbf{L}. \tag{14}$$

The term $\mathbf{L}^{\mathrm{T}}\mathbf{L}$ can be neglected because, under the Euler–Bernoulli beam theory that assumes small strains, $(s' - 1)$ and $Y\theta'$ in $\mathbf{L}$ are small. Note that E_{XX} is the only non-zero strain component.

3. Displacement interpolations

Consider a 2D beam element of length L in the XY plane shown in Fig. 2. The element has two end nodes and one auxiliary node at its center. There are three displacement fields to be interpolated, i.e., u_X, u_Y, and θ. The strategy used to obtain the field consistency is to explicitly describe the interpolations of only two of the three fields. After that, the interpolation of the last field is obtained by employing the dependent relationship between these three fields defined by Eq. (6). Here, u_X and u_Y are selected to be explicitly interpolated by polynomials. Define the displacement vector $\mathbf{u}$ as

$$\mathbf{u} = \begin{Bmatrix} u_X \\ u_Y \end{Bmatrix} = \mathbf{P}^{\mathrm{T}}\mathbf{A}, \tag{15}$$

where

$$\mathbf{P} = \begin{bmatrix} 1 & X & X^2 & 0 & 0 & 0 & 0 \\ 0 & 0 & 0 & 1 & X & X^2 & X^3 \end{bmatrix}^{\mathrm{T}}, \tag{16}$$

$$\mathbf{A} = [a_0 \;\; a_1 \;\; a_2 \;\; b_0 \;\; b_1 \;\; b_2 \;\; b_3]^{\mathrm{T}}. \tag{17}$$

Here, $\mathbf{P}$ holds polynomial bases while $\mathbf{A}$ contains their coefficients.

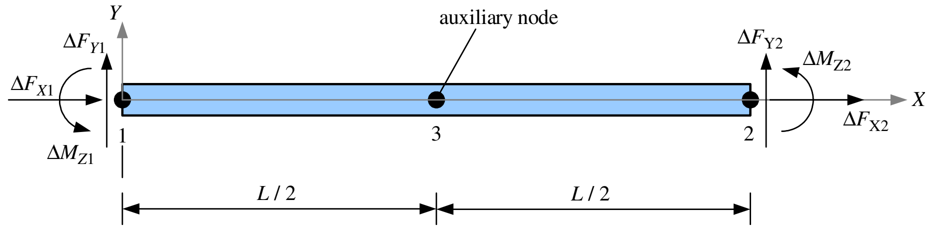

Fig. 2. Proposed beam element.

Define the nodal displacement vector **U** and the nodal force vector **f** as

$$\mathbf{U} = [u_{X1} \;\; u_{Y1} \;\; \theta_{Z1} \;\; u_{X2} \;\; u_{Y2} \;\; \theta_{Z2} \;\; u_{X3}]^{\mathrm{T}}, \tag{18}$$

$$\mathbf{f} = [F_{X1} \;\; F_{Y1} \;\; M_{Z1} \;\; F_{X2} \;\; F_{Y2} \;\; M_{Z2} \;\; 0]^{\mathrm{T}}. \tag{19}$$

The number subscripts represent node numbers. The last degree of freedom at the center of the element is introduced only to increase the order of the interpolation of the axial displacement. The applied force is not allowed at the center node. As a result, for the user, the element has only two nodes.

From Eq. (15), with help of Eq. (6), the degrees of freedom can be expressed as

$$u_{X1} = a_0, \tag{20}$$

$$u_{Y1} = b_0, \tag{21}$$

$$\theta_{Z1} = \tan^{-1}\left(\frac{u'_Y(0)}{1 + u'_X(0)}\right) = \tan^{-1}\left(\frac{b_1}{1 + a_1}\right), \tag{22}$$

$$u_{X2} = a_0 + a_1 L + a_2 L^2, \tag{23}$$

$$u_{Y2} = b_0 + b_1 L + b_2 L^2 + b_3 L^3, \tag{24}$$

$$\begin{aligned}\theta_{Z2} &= \tan^{-1}\left(\frac{u'_Y(L)}{1 + u'_X(L)}\right) \\ &= \tan^{-1}\left(\frac{b_1 + 2b_2 L + 3b_3 L^2}{1 + a_1 + 2a_2 L}\right),\end{aligned} \tag{25}$$

$$u_{X3} = a_0 + a_1 \frac{L}{2} + a_2 \frac{L^2}{4}. \tag{26}$$

By using Eqs. (20)–(26), the coefficients in Eq. (17) are expressed in terms of the nodal degrees of freedom as

$$a_0 = u_{X1}, \tag{27}$$

$$a_1 = -\frac{3u_{X1} + u_{X2} - 4u_{X3}}{L}, \tag{28}$$

$$a_2 = \frac{2(u_{X1} + u_{X2} - 2u_{X3})}{L^2}, \tag{29}$$

$$b_0 = u_{Y1}, \tag{30}$$

$$b_1 = \frac{1}{L}(L - 3u_{X1} - u_{X2} + 4u_{X3}) \tan\theta_{Z1}, \tag{31}$$

$$\begin{aligned}b_2 = -\frac{1}{L^2}[&3(u_{Y1} - u_{Y2}) + 2(L - 3u_{X1} - u_{X2} + 4u_{X3}) \\ &\times \tan\theta_{Z1} + (L + u_{X1} + 3u_{X2} - 4u_{X3}) \tan\theta_{Z2}],\end{aligned} \tag{32}$$

$$\begin{aligned}b_3 = \frac{1}{L^3}[&2(u_{Y1} - u_{Y2}) + (L - 3u_{X1} - u_{X2} + 4u_{X3}) \tan\theta_{Z1} \\ &+ (L + u_{X1} + 3u_{X2} - 4u_{X3}) \tan\theta_{Z2}].\end{aligned} \tag{33}$$

Consequently, the displacements can be expressed as

$$\begin{aligned}u_X = u_{X1} &- \frac{X}{L}[3u_{X1} + u_{X2} - 4u_{X3}] \\ &+ \frac{X^2}{L^2}[2(u_{X1} + u_{X2} - 2u_{X3})],\end{aligned} \tag{34}$$

$$\begin{aligned}u_Y = u_{Y1} &+ \frac{X}{L}[(L - 3u_{X1} - u_{X2} + 4u_{X3}) \tan\theta_{Z1}] \\ &- \frac{X^2}{L^2}[3(u_{Y1} - u_{Y2}) + 2(L - 3u_{X1} - u_{X2} + 4u_{X3}) \\ &\times \tan\theta_{Z1} + (L + u_{X1} + 3u_{X2} - 4u_{X3}) \tan\theta_{Z2}] \\ &+ \frac{X^3}{L^3}[2(u_{Y1} - u_{Y2}) + (L - 3u_{X1} - u_{X2} + 4u_{X3}) \\ &\times \tan\theta_{Z1} + (L + u_{X1} + 3u_{X2} - 4u_{X3}) \tan\theta_{Z2}].\end{aligned} \tag{35}$$

In contrast to conventional displacement interpolations, it can be seen that the displacements are not linear functions of the degrees of freedom. Note that Eqs. (34) and (35) are derived with the help of Eq. (6). The interpolation expressions related to θ can be obtained by appropriately considering Eqs. (4)–(6) together with Eqs. (34) and (35). In this way, the dependent relationship between u_X, u_Y, and θ is ensured.

4. Derivation of the nonlinear stiffness matrix equation

Consider the virtual work equation for the total Lagrangian formulation written as

$$\begin{aligned}&\int_0^L \int_A S_{XX} \delta E_{XX} \, \mathrm{d}A \, \mathrm{d}X \\ &= \int_0^L \int_A E E_{XX} \delta E_{XX} \, \mathrm{d}A \, \mathrm{d}X \\ &= \sum_{I=1}^{2} F_{XI} \delta u_{XI} + \sum_{I=1}^{2} F_{YI} \delta u_{YI} + \sum_{I=1}^{2} M_{ZI} \delta \theta_{ZI} \\ &\quad + \int_0^L p_X \delta u_X \, \mathrm{d}X + \int_0^L p_Y \delta u_Y \, \mathrm{d}X.\end{aligned} \tag{36}$$

Here, S_{XX} is the XX component of the second Piola–Kirchhoff stresses and is related to the Green strain E_{XX} through the Young's modulus E. The cross-sectional area of the beam is denoted as A. Moreover, p_X and p_Y denote the distributed axial and transverse loads, respectively.

From Eq. (14), the virtual Green strain can be expressed as

$$\begin{aligned}\delta E_{XX} &= \delta[(1+u'_X)\cos\theta + u'_Y\sin\theta - Y\theta' - 1] \\ &= \cos\theta\delta u'_X - (1+u'_X)\sin\theta\delta\theta + \sin\theta\delta u'_Y \\ &\quad + u'_Y\cos\theta\delta\theta - Y\delta\theta' \\ &= \cos\theta\delta u'_X + \sin\theta\delta u'_Y - Y\delta\theta'.\end{aligned} \tag{37}$$

Hence, the internal virtual work is expressed as

$$\begin{aligned}&\int_0^L\int_A EE_{XX}\delta E_{XX}\,\mathrm{d}A\,\mathrm{d}X \\ &= \int_0^L\int_A E[s' - Y\theta' - 1][\cos\theta\delta u'_X \\ &\quad + \sin\theta\delta u'_Y - Y\delta\theta']\,\mathrm{d}A\,\mathrm{d}X \\ &= EA\int_0^L s'\cos\theta\delta u'_X\,\mathrm{d}X + EA\int_0^L s'\sin\theta\delta u'_Y\,\mathrm{d}X \\ &\quad - EA\int_0^L \cos\theta\delta u'_X\,\mathrm{d}X \\ &\quad - EA\int_0^L \sin\theta\delta u'_Y\,\mathrm{d}X + EI\int_0^L \theta'\delta\theta'\,\mathrm{d}X \\ &= EA\int_0^L (1+u'_X)\delta u'_X\,\mathrm{d}X + EA\int_0^L u'_Y\delta u'_Y\,\mathrm{d}X \\ &\quad - EA\int_0^L \cos\theta\delta u'_X\,\mathrm{d}X - EA\int_0^L \sin\theta\delta u'_Y\,\mathrm{d}X \\ &\quad + EI\int_0^L \theta'\delta\theta'\,\mathrm{d}X.\end{aligned} \tag{38}$$

By using Eqs. (4) and (6), θ' is derived as

$$\theta' = \frac{(1+u'_X)u''_Y - u'_Y u''_X}{(1+u'_X)^2 + (u'_Y)^2}. \tag{39}$$

The internal virtual work then becomes

$$\begin{aligned}&\int_0^L\int_A EE_{XX}\delta E_{XX}\,\mathrm{d}A\,\mathrm{d}X \\ &= EA\int_0^L (1+u'_X)\delta u'_X\,\mathrm{d}X + EA\int_0^L u'_Y\delta u'_Y\,\mathrm{d}X \\ &\quad - EA\int_0^L \frac{1+u'_X}{\sqrt{(1+u'_X)^2 + (u'_Y)^2}}\delta u'_X\,\mathrm{d}X \\ &\quad - EA\int_0^L \frac{u'_Y}{\sqrt{(1+u'_X)^2 + (u'_Y)^2}}\delta u'_Y\,\mathrm{d}X \\ &\quad + EI\int_0^L \frac{(1+u'_X)u''_Y - u'_Y u''_X}{(1+u'_X)^2 + (u'_Y)^2}\delta\theta'\,\mathrm{d}X.\end{aligned} \tag{40}$$

Define vectors $\mathbf{N}_X$ and $\mathbf{N}_Y$ as

$$\mathbf{N}_X = \left[\frac{\partial u_X}{\partial u_{X1}}\ \frac{\partial u_X}{\partial u_{Y1}}\ \frac{\partial u_X}{\partial \theta_{Z1}}\ \frac{\partial u_X}{\partial u_{X2}}\ \frac{\partial u_X}{\partial u_{Y2}}\ \frac{\partial u_X}{\partial \theta_{Z2}}\ \frac{\partial u_X}{\partial u_{X3}}\right], \tag{41}$$

$$\mathbf{N}_Y = \left[\frac{\partial u_Y}{\partial u_{X1}}\ \frac{\partial u_Y}{\partial u_{Y1}}\ \frac{\partial u_Y}{\partial \theta_{Z1}}\ \frac{\partial u_Y}{\partial u_{X2}}\ \frac{\partial u_Y}{\partial u_{Y2}}\ \frac{\partial u_Y}{\partial \theta_{Z2}}\ \frac{\partial u_Y}{\partial u_{X3}}\right]. \tag{42}$$

The virtual translational displacements and their derivatives are then written as

$$\delta u_X = \mathbf{N}_X\delta\mathbf{U}, \quad \delta u_Y = \mathbf{N}_Y\delta\mathbf{U}, \tag{43}$$

$$\delta u'_X = \mathbf{N}'_X\delta\mathbf{U}, \quad \delta u'_Y = \mathbf{N}'_Y\delta\mathbf{U}. \tag{44}$$

Note that $\mathbf{N}_X$, $\mathbf{N}_Y$, $\mathbf{N}'_X$ and $\mathbf{N}'_Y$ can be derived from Eqs. (34) and (35).

By using Eqs. (4), (6) and (44), the virtual rotational displacement and its derivative can be derived as

$$\begin{aligned}\delta\theta &= -\frac{u'_Y}{\left(1+u'_X\right)^2 + (u'_Y)^2}\delta u'_X + \frac{1+u'_X}{(1+u'_X)^2 + (u'_Y)^2}\delta u'_Y \\ &= \left[-\frac{u'_Y}{(1+u'_X)^2 + (u'_Y)^2}\mathbf{N}'_X + \frac{1+u'_X}{(1+u'_X)^2 + (u'_Y)^2}\mathbf{N}'_Y\right] \\ &\quad \times \delta\mathbf{U} \\ &= \mathbf{N}_\theta\delta\mathbf{U},\end{aligned} \tag{45}$$

$$\delta\theta' = \mathbf{N}'_\theta\delta\mathbf{U}. \tag{46}$$

Finally, by using Eqs. (40), (44), and (46) in Eq. (36), the nonlinear stiffness equation is obtained as

$$\mathbf{\Phi}(\mathbf{U}) = \mathbf{f}, \tag{47}$$

where

$$\begin{aligned}\mathbf{\Phi}(\mathbf{U}) &= EA\int_0^L (1+u'_X){\mathbf{N}'_X}^{\mathrm{T}}\,\mathrm{d}X + EA\int_0^L u'_Y{\mathbf{N}'_Y}^{\mathrm{T}}\,\mathrm{d}X \\ &\quad - EA\int_0^L \frac{1+u'_X}{\sqrt{(1+u'_X)^2 + (u'_Y)^2}}{\mathbf{N}'_X}^{\mathrm{T}}\,\mathrm{d}X \\ &\quad - EA\int_0^L \frac{u'_Y}{\sqrt{(1+u'_X)^2 + (u'_Y)^2}}{\mathbf{N}'_Y}^{\mathrm{T}}\,\mathrm{d}X \\ &\quad + EI\int_0^L \frac{(1+u'_X)u''_Y - u'_Y u''_X}{(1+u'_X)^2 + (u'_Y)^2}{\mathbf{N}'_\theta}^{\mathrm{T}}\,\mathrm{d}X \\ &\quad - \int_0^L \mathbf{N}_X^{\mathrm{T}} p_X\,\mathrm{d}X - \int_0^L \mathbf{N}_Y^{\mathrm{T}} p_Y\,\mathrm{d}X.\end{aligned} \tag{48}$$

Note that derivatives of u_X and u_Y can be derived from Eqs. (34) and (35). It can be seen that Eq. (47) is nonlinear. In this study, the Newton–Raphson method is employed to solve this nonlinear equation.

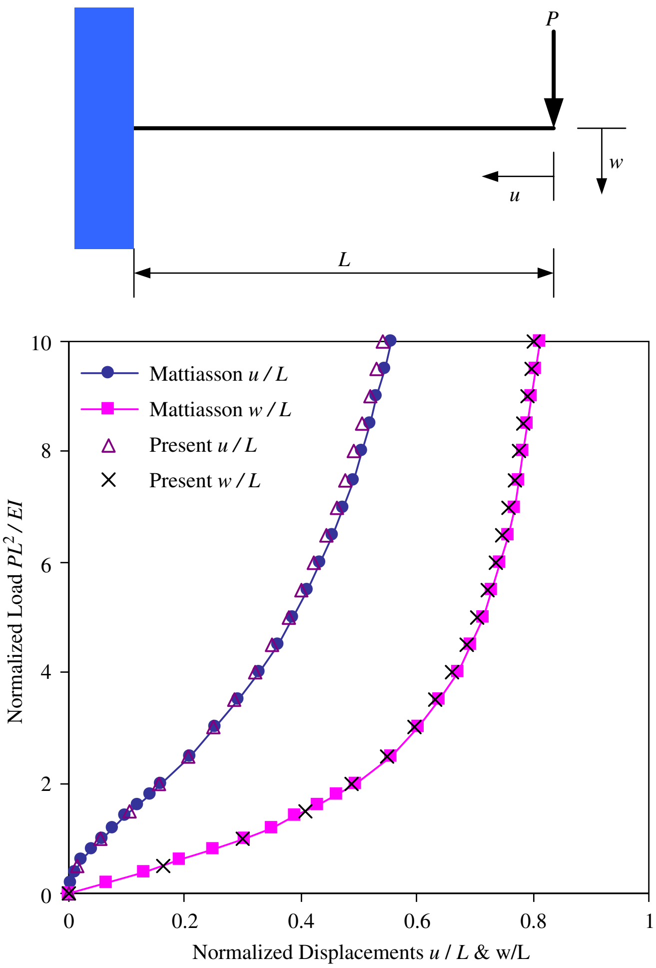

Fig. 3. Cantilever beam with an end point load.

5. Results

The following four examples are used to illustrate the validity and efficiency of the proposed beam element. The results obtained from this study are compared with the existing results in the literature.

5.1. Cantilever beam with an end point load

The first problem to be considered is a cantilever beam subjected to a concentrated load at the free end as shown in Fig. 3. In this problem, five elements are used to model the beam. The obtained results are compared with the elliptic integral solutions by Mattiasson [23] in Fig. 3 and, in numeric form, in Table 1. The results indicate good agreement between the present solutions and Mattiasson's solutions.

5.2. Cantilever beam with an end moment

A cantilever beam in this example is subjected to a concentrated end moment as shown in Fig. 4. This problem has been used by many researchers for testing nonlinear beam elements since the analytical solutions for the problem exist. Examples include works by Filho and Awruch [24], who solved the problem by using 160 eight-noded hexahedral isoparametric elements, and by Shi and Voyiadjis [25], who used 10 four-noded plate elements. In this study, the problem is solved with only

Table 1
Cantilever beam with an end point load

$\frac{PL^2}{EI}$	u/L		w/L	
	Mattiasson [23]	Present study	Mattiasson [23]	Present study
1.0	0.05643	0.05559	0.30172	0.29946
2.0	0.16064	0.15672	0.49346	0.48748
3.0	0.25442	0.24757	0.60325	0.59534
4.0	0.32894	0.32003	0.66996	0.66126
5.0	0.38763	0.37733	0.71379	0.70479
6.0	0.43459	0.42335	0.74457	0.73550
7.0	0.47293	0.46103	0.76737	0.75831
8.0	0.50483	0.49245	0.78498	0.77597
9.0	0.53182	0.51909	0.79906	0.79011
10.0	0.55500	0.54199	0.81061	0.80173

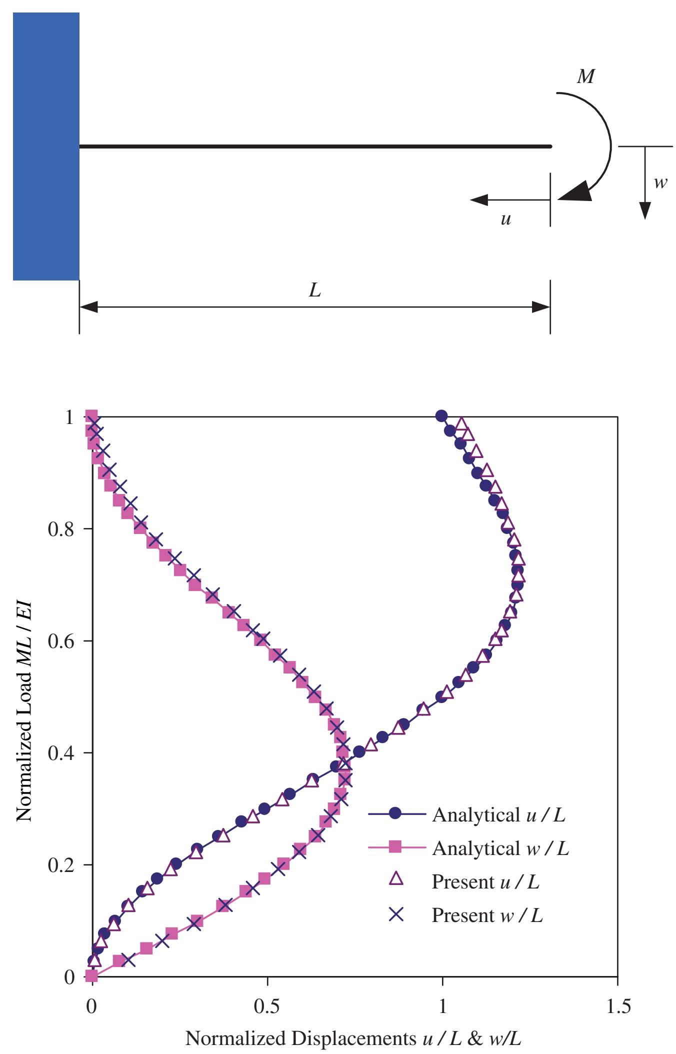

Fig. 4. Cantilever beam with an end moment.

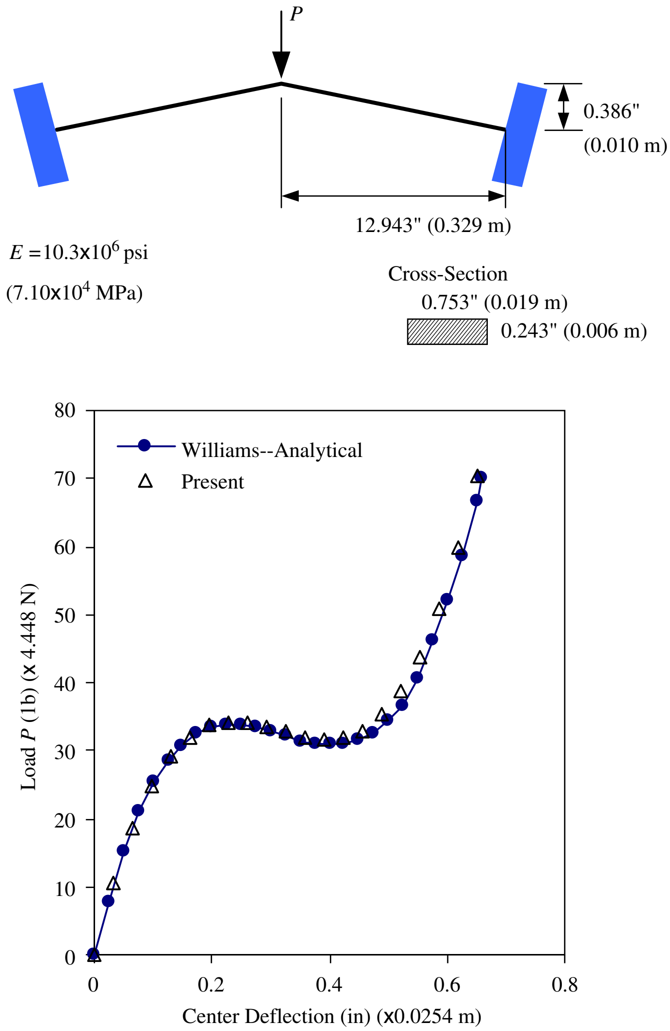

Fig. 5. Williams' toggle.

five elements. The results obtained from this study are compared with the analytical solutions in Fig. 4. It can be seen from the comparison that good agreement between the present solutions and the analytical solutions is obtained.

5.3. Williams' toggle frame

A frame in Fig. 5 was first solved analytically and experimentally by Williams [26]. It is sufficient to consider only half of the frame since the problem is symmetric. The problem is considered as a good benchmark for testing new nonlinear beam elements and it has been investigated by many researchers [1,27,28]. Wood and Zienkiewicz [1] solved the problem by using five six-noded paralinear isoparametric elements per member. Yang and Chiou [28] employed five two-noded beam elements per member. In this study, the problem is analyzed by using only two elements per member. The result obtained from this study is compared with the analytical solution by Williams [26] in Fig. 5. Good agreement between the present and analytical solutions is observed.

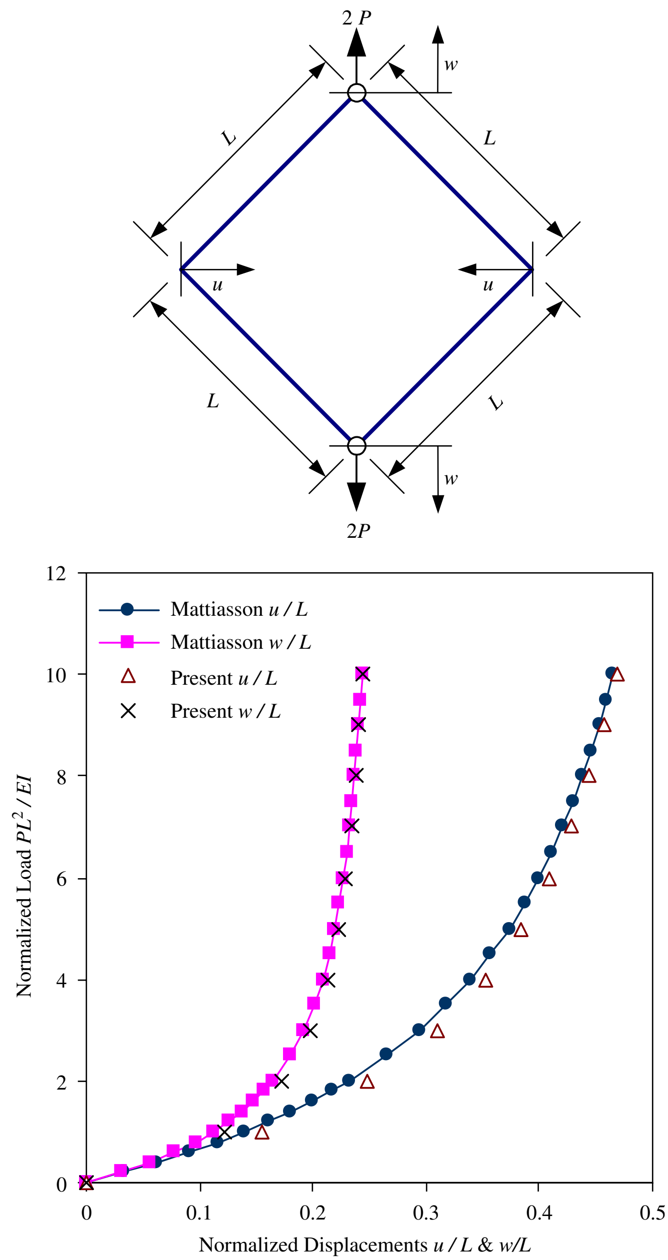

Fig. 6. Pinned-fixed square diamond frame in tension.

5.4. Pinned-fixed square diamond frame in tension

A pinned-fixed square diamond frame is loaded in tension as shown in Fig. 6. Since the problem is symmetric, only half of the diamond is analyzed. The problem is analyzed by using two elements per member. The results are compared with those from Mattiasson [23] in Fig. 6 and, in numeric form, in Table 2. Good agreement between the present and Mattiasson's results can be observed from the comparison.

6. Conclusions

In this study, a new 2D field-consistent Euler–Bernoulli beam element for large displacement analysis with small strains using

Table 2
Pinned-fixed square diamond frame in tension

$\frac{PL^2}{EI}$	u/L		w/L	
	Mattiasson [23]	Present study	Mattiasson [23]	Present study
1.0	0.13960	0.15592	0.11252	0.12276
2.0	0.23184	0.24894	0.16429	0.17228
3.0	0.29447	0.30958	0.19183	0.19750
4.0	0.33940	0.35211	0.20839	0.21238
5.0	0.37322	0.38367	0.21931	0.22211
6.0	0.39966	0.40810	0.22703	0.22895
7.0	0.42097	0.42765	0.23279	0.23405
8.0	0.43855	0.44370	0.23726	0.23801
9.0	0.45335	0.45716	0.24084	0.24120
10.0	0.46601	0.46865	0.24380	0.24383

the total Lagrangian formulation is proposed. When the total Lagrangian formulation is used to formulate beam elements for large displacement analysis, it is difficult to find a set of interpolations that are field consistent. This is unfortunately because of the intrinsic complex relationships between the relevant displacements. As a result, performances of total Lagrangian beam elements are unnecessarily degraded by field-inconsistent interpolations. If interpolations that are field consistent can be found, better performances of total Lagrangian beam elements can be expected. For the 2D Euler–Bernoulli beam element proposed in this study, there are three displacement fields to be interpolated, i.e., the axial displacement, transverse displacement, and rotation. The interpolations for the axial and transverse displacements are described first by using polynomials. Subsequently, the interpolation for the rotation is derived from the dependent relationship between the three displacement fields. Thus, the problem of field inconsistency is avoided and the proposed element eliminates this disadvantage of the total Lagrangian formulation. The obtained interpolations are found to be nonlinear functions of nodal degrees of freedom. From the comparison with the existing problems in the literature, it can be seen that the proposed element is capable of giving accurate results by using small numbers of elements. This confirms the validity and efficiency of the proposed element.

References

[1] R.D. Wood, O.C. Zienkiewicz, Geometrically nonlinear finite element analysis of beams, frames, arches and axisymmetric shells, Comput. Struct. 7 (1977) 725–735.
[2] K.-J. Bathe, S. Bolourchi, Large displacement analysis of three-dimensional beam structures, Int. J. Numer. Methods Eng. 14 (1979) 961–986.
[3] M.A. Crisfield, A consistent co-rotational formulation for non-linear, three-dimensional, beam-elements, Comput. Methods Appl. Mech. Eng. 81 (1990) 131–150.
[4] M. Saje, A variational principle for finite planar deformation of straight slender elastic beams, Int. J. Solids Struct. 26 (1990) 887–900.
[5] Y.-B. Yang, L.-J. Leu, Force recovery procedures in nonlinear analysis, Comput. Struct. 41 (1991) 1255–1261.
[6] M. Saje, G. Turk, A. Kalagasidu, B. Vratanar, A kinematically exact finite element formulation of elastic–plastic curved beams, Comput. Struct. 67 (1998) 197–214.
[7] L.H. Teh, M.J. Clarke, Co-rotational and Lagrangian formulations for elastic three-dimensional beam finite elements, J. Const. Steel Res. 48 (1998) 123–144.
[8] K.M. Hsiao, J.Y. Lin, W.Y. Lin, A consistent co-rotational finite element formulation for geometrically nonlinear dynamic analysis of 3-D beams, Comput. Methods Appl. Mech. Eng. 169 (1999) 1–18.
[9] E. Yamaguchi, W. Kanok-Nukulchai, M. Hammadeh, Y. Kubo, Simple degenerate formulation for large displacement analysis of beams, J. Eng. Mech. 125 (1999) 1140–1146.
[10] P.F. Pai, T.J. Anderson, E.A. Wheater, Large-deformation tests and total-Lagrangian finite-element analyses of flexible beams, Int. J. Solids Struct. 37 (2000) 2951–2980.
[11] M. Schulz, F.C. Filippou, Non-linear spatial Timoshenko beam element with curvature interpolation, Int. J. Numer. Methods Eng. 50 (2001) 761–785.
[12] Y.B. Yang, S.R. Kuo, Y.S. Wu, Incrementally small-deformation theory for nonlinear analysis of structural frames, Eng. Struct. 24 (2002) 783–798.
[13] J.N. Reddy, On locking-free shear deformable beam finite elements, Comput. Methods Appl. Mech. Eng. 149 (1997) 113–132.
[14] J.N. Reddy, C.M. Wang, K.H. Lee, Relationships between bending solutions of classical and shear deformation beam theories, Int. J. Solids Struct. 34 (1997) 3373–3384.
[15] M. Ganapathi, B.P. Patel, J. Saravanan, M. Touratier, Shear flexible curved spline beam element for static analysis, Finite Elem. Anal. Des. 32 (1999) 181–202.
[16] K.-J. Bathe, Finite Element Procedures in Engineering Analysis, Prentice-Hall, Englewood Cliffs, NJ, 1982.
[17] E.N. Dvorkin, E. Onate, J. Oliver, On a non-linear formulation for curved Timoshenko beam elements considering large displacement/rotation increments, Int. J. Numer. Methods Eng. 26 (1988) 1597–1613.
[18] K.S. Surana, R.M. Sorem, Geometrically non-linear formulation for three dimensional curved beam elements with large rotations, Int. J. Numer. Methods Eng. 28 (1989) 43–73.
[19] Y.-B. Yang, W. McGuire, Stiffness matrix for geometric nonlinear analysis, J. Struct. Eng. 112 (1986) 853–877.
[20] M.A. Crisfield, G.F. Moita, A unified co-rotational framework for solids, shells and beams, Int. J. Solids Struct. 33 (1996) 2969–2992.
[21] A. Eriksson, C. Pacoste, Symbolic software tools in the development of finite elements, Comput. Struct. 72 (1999) 579–593.
[22] C. Pacoste, A. Eriksson, Beam elements in instability problems, Comput. Methods Appl. Mech. Eng. 144 (1997) 163–197.
[23] K. Mattiasson, Numerical results from large deflection beam and frame problems analysed by means of elliptic integrals, Int. J. Numer. Methods Eng. 17 (1981) 145–153.
[24] L.A.D. Filho, A.M. Awruch, Geometrically nonlinear static and dynamic analysis of shells and plates using the eight-node hexahedral element with one-point quadrature, Finite Elem. Anal. Des. 40 (2004) 1297–1315.
[25] G. Shi, G.Z. Voyiadjis, Geometrically nonlinear analysis of plates by assumed strain element with explicit tangent stiffness matrix, Comput. Struct. 41 (1991) 757–763.
[26] F.W. Williams, An approach to the nonlinear behaviour of the members of a rigid jointed plane framework with finite deflections, Q. J. Mech. Appl. Math. 17 (1964) 451–469.
[27] M. Papadrakakis, Post-buckling analysis of spatial structures by vector iteration methods, Comput. Struct. 14 (1981) 393–402.
[28] Y.-B. Yang, H.-T. Chiou, Rigid body motion test for nonlinear analysis with beam elements, J. Eng. Mech. 113 (1987) 1404–1419.